Ab initio and scanning tunneling microscopy study of an indium-terminated GaAs(100) surface: An indium-induced surface reconstruction change in the $c(8\times2)$ structure

J. J. K. Lång,[1,*] M. P. J. Punkkinen,[1,2] P. Laukkanen,[1,3] M. Kuzmin,[1,4] V. Tuominen,[1] M. Pessa,[3] M. Guina,[3] I. J. Väyrynen,[1] K. Kokko,[1] B. Johansson,[2,5] and L. Vitos[2,5,6]

[1]*Department of Physics and Astronomy, University of Turku, FI-20014 Turku, Finland*

[2]*Applied Materials Physics, Department of Materials Science and Engineering, Royal Institute of Technology, SE-10044 Stockholm, Sweden*

[3]*Optoelectronics Research Centre, Tampere University of Technology, FI-33101 Tampere, Finland*

[4]*Ioffe Physical-Technical Institute of the Russian Academy of Sciences, St. Petersburg 194021, Russian Federation*

[5]*Condensed Matter Theory Group, Physics Department, Uppsala University, SE-75121 Uppsala, Sweden*

[6]*Research Institute for Solid State Physics and Optics, P.O. Box 49, H-1525 Budapest, Hungary*

(Received 10 March 2010; revised manuscript received 22 April 2010; published 7 June 2010)

Technologically useful indium- (In) terminated $c(8\times2)$-reconstructed GaAs(100) substrate surface has been studied by first-principles calculations and scanning tunneling microscopy (STM) measurements. Our total-energy calculations demonstrate the stability of four different so-called ζa structures with In monomer rows and In coverage between 0.5 and 2 monolayers on the GaAs(100) substrate. Thus, we introduce a surface system, which stabilizes the ζa reconstruction. Furthermore, an interesting trend is found. Atomic structure of the $c(8\times2)$ reconstruction depends on the surface-layer cation and substrate volumes, which, in principle, allows to tune the surface structure by cation adsorption. This phenomenon is related to the peculiar $c(8\times2)$ atomic surface structure, which shows mixed surface layer, including both anions and cations, and uncommon metallic-type cations in the ζa structure, which do not show covalent bonds. Our results predict a structural transition from the ζ structure to the ζa structure as the surface cation size is increased at 0 K. The found transition is probably related to the disordered surface structures (consisting of ζ and ζa building blocks) found experimentally by x-ray diffraction at room temperature. Comparison of the STM images, calculated for various $c(8\times2)$ models, with the former and present measured STM images of In/GaAs(100)$c(8\times2)$ supports the presence of stable ζa reconstructions.

DOI: 10.1103/PhysRevB.81.245305 PACS number(s): 68.35.−p, 81.10.−h, 73.20.−r, 68.47.Fg

I. INTRODUCTION

Considering the development of epitaxially grown III-V compound semiconductor heterojunction devices, the surface properties of the growth front play a substantial role (e.g., Refs. 1–6). In addition to that, for the realization of III-V channel metal-insulator-semiconductor (MIS) transistor, it is essential to understand and manipulate the starting III-V surface properties for the insulator growth.[7–17]

Adding a small amount of indium [about 1 monolayer (ML)], which causes an In-stabilized $c(8\times2)$-reconstructed (100) surface on the heteroepitaxial III-V growth front (e.g., InP/InGaAs and InAs/GaSb), has been found to improve the properties of these interfaces for electronics devices.[1,18–20] For example, Anan *et al.*[1] observed even 100-fold improvement in photoluminescence (PL) intensity for III-P/III-As heterostructure, in the growth of which about 1 ML of In was deposited before the P_2 exposure and III-P layer growth [thus producing In-induced $c(8\times2)/(4\times2)$ structure on the III-As surface as deduced by reflection high-energy electron diffraction (RHEED)], compared to the structure grown without the In prelayer. It is worth noting that usually the PL intensity is inversely proportional to the threshold current density of laser diodes. We also note that the $c(8\times2)$ and (4×2) reconstructions are structurally very close to each other, and that often it is difficult to distinguish the $c(8\times2)$ from (4×2) geometry in measurements. Hereafter in this paper, the $c(8\times2)$ means the both geometries. Furthermore, InAs/GaAs heterostructure is known to follow the Stranski-Krastanov growth mode, where the critical thickness of InAs wetting layer is about 2 ML due to large lattice mismatch between InAs and GaAs.[21,22] However, under In-rich growth conditions, the critical thickness can be substantially increased, and the resulted interface reveals superior quality and notably improved PL intensity.[21–23] Moreover, the In-stabilized $c(8\times2)$ surface has been used as a starting substrate for producing insulator/III-V interfaces for MIS transistors.[17,24] For example, in the case of InGaAs, indium atoms tend to occupy surface-layer sites, leading to the In-terminated $c(8\times2)$-reconstructed surface of InGaAs under As-deficient surface-cleaning conditions. To understand the reasons for the beneficial effects of the In-terminated $c(8\times2)$ reconstructions and to controllably utilize these surfaces, it is essential to know the atomic structures and properties of the In/III-V(100)$c(8\times2)$ surfaces. The specific surface structure has in general profound implications concerning, e.g., different kinds of adsorption and desorption phenomena, which are important for applications.

In general, the $c(8\times2)$ surfaces have been found to be composed of unique ζ structural units,[25–34] which include dimers in the subsurface rather than top layer (Fig. 1). Earlier, various models were proposed for the group-III-rich $c(8\times2)$ reconstruction, including $\beta(4\times2)$ structures with the group III dimers, which are counterparts to the famous $\beta(2\times4)$ reconstructions found in the group-V-rich conditions on many III-V surfaces. However, Lee *et al.* introduced

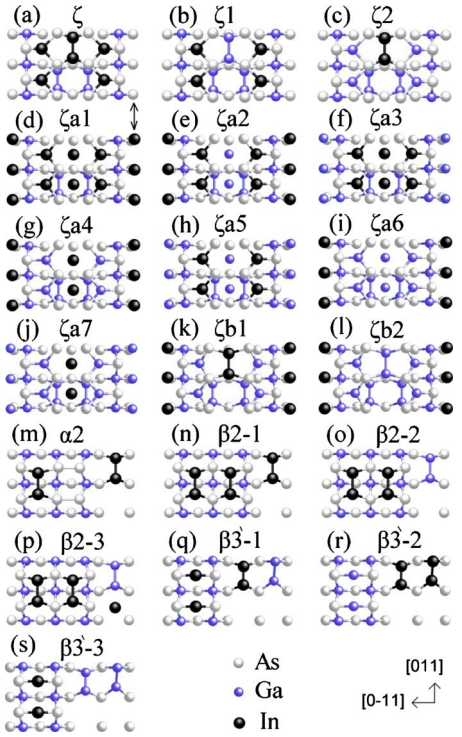

FIG. 1. (Color online) (a)–(s) Atomic models for the In/GaAs(100)$c(8\times2)$ surface.

an unusual atomic structure, referred to as the "ζ" model, which led to the lowest total energy and good agreement between the experimental and theoretical STM images.[25] Kumpf *et al.* put forward an atomic structure, which was a generalization of the ζ model in the sense that it allowed two different types of local configurations for the cation atoms.[26,27] The inherent feature of this model is partial disorder. This model leads to atomic structure similar to the ζ presented by Lee *et al.* for GaAs (*The model is only slightly different from the one proposed on the basis of theoretical considerations by Lee et al.*[27]) whereas the ratio of the occupations of the different local configurations for the cation atoms is significantly different for InAs, InSb being between GaAs and InAs concerning these occupations.[26,27] Miwa *et al.* considered an atomic structure "ζa," which is an ordered variant of the atomic model introduced by Kumpf *et al.* including only those local configurations which were excluded in the original ζ atomic structure.[28] Therefore, the ζ and ζa atomic models include 0% (for ζ) and 100% (for ζa) occupations for the monomer rows marked by an arrow and shown in Figs. 1(a) and 1(d). Additionally, there is a top-layer group III dimer in the ζ structure whereas two non-dimerized group III adatoms in the ζa structure. The partially disordered areas, which were detected by surface x-ray diffraction, may be thought as microscopic mixtures of the ordered ζ and ζa reconstructions. Furthermore, the relative [011] displacements of the ζ or ζa cells cause the $c(8\times2)$ periodicity. One should note that "ζ-kind" areas (ζ or ζa) have been found to form on III-V's without significant disorder related to the partial occupancy, as can be deduced from the scanning-tunneling-microscopy (STM) and atomic force microscopy results.[30,33–35] Interestingly, Kolodziej *et al.* reported a well-ordered ζa structure for InSb.[33] However, according to Miwa *et al.*, only the ζ phase is energetically stable for InAs (as for GaAs).[28]

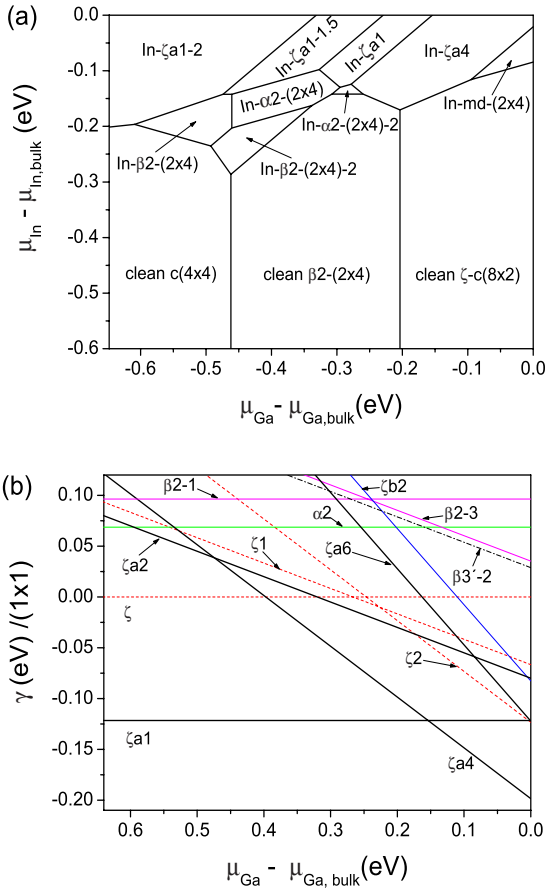

FIG. 2. (Color online) (a) Surface phase diagrams for the In/GaAs(100) surface. (b) Energy diagram of the In/GaAs(100) surface in the In-rich limit $\mu_{In}=\mu_{In,bulk}$. Please see the models in Fig. 1. For clarity, the phase diagram does not include all models that were calculated.

In this paper, we report the energetic stability of ζa structures, with varying amounts of In on the In/GaAs(100)$c(8\times2)$ surface by *ab initio* total-energy calculations. The comparison of the calculated STM images for various $c(8\times2)$ models with the former[35] and present measured images of In/GaAs(100)$c(8\times2)$ supports the presence of these stable ζa reconstructions. It is shown that the adsorbed atom and substrate types have a significant effect on the relative stabilities of the ζ and ζa structures, and a structural transition with the increasing cation size at 0 K is predicted. These results also explain nicely the different occupations for the local configurations on different III-V semiconductor surfaces found experimentally.[26,27] It is possible that the specific atomic structure of the In/GaAs(100)$c(8\times2)$ surface is related to the above-mentioned useful effects of In-terminated substrates concerning the development of device materials.

II. METHODS

Calculations were performed using an *ab initio* density functional total-energy method within the local-density

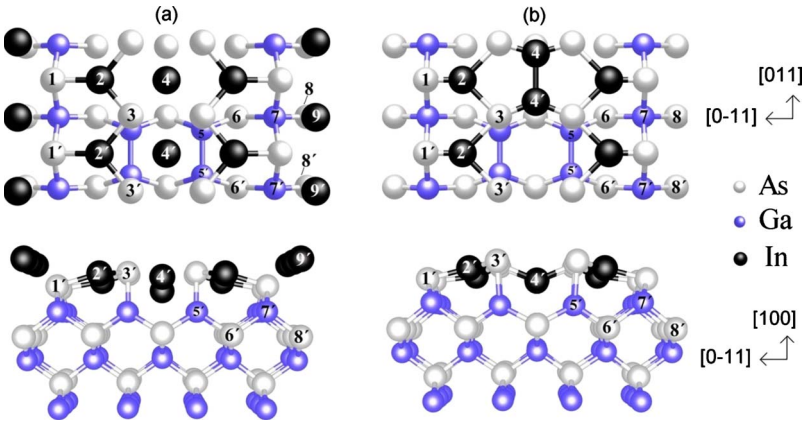

FIG. 3. (Color online) (a) ζa and (b) ζ reconstruction of the In/GaAs(100)$c(8\times2)$ surface [Figs. 1(a) and 1(d)]. Some atoms are numbered to facilitate comparison of bond lengths (Table IV).

approximation.[36,37] The approach is based on plane-wave basis and projector-augmented wave method[38,39] (Vienna *ab initio* simulation package, VASP).[40–43] The optimization of the atomic structure was performed using conjugate-gradient minimization of the total energy with respect to the atomic coordinates. The GaAs(100) and In/GaAs(100) surfaces were simulated using (2×4) and (4×2) slabs of 12 atomic layers, separated by a vacuum of 23 Å wide. The (8×2) slabs were also used to simulate the experimentally found $c(8\times2)$ structure but the effect of the double periodicity on total energy is marginal [affecting the relative surface energies less than 1 meV per (1×1) surface area]. The dangling bonds of the bottom surface Ga atoms were passivated by fractionally charged pseudohydrogen atoms ($Z=1.25$) and two bottom layers of the slabs were fixed to ideal bulk positions. Other atoms including pseudohydrogens were relaxed until the remaining forces were less than 20 meV/Å. The number of k points in the Brillouin zone was eight corresponding to 64 k points in the Brillouin zone of the (1×1) slab. The k-point sampling was performed by the Monkhorst-Pack scheme[44] with the origin shifted to the Γ point. The plane-wave cutoff energy was 300 eV. Theoretical lattice constant of 5.63 Å was obtained and used for GaAs (about 6.06 Å for GaSb and InAs and 6.47 Å for InSb). The constant-current STM images were simulated within the Tersoff-Hamann approximation.[45]

Thermodynamically the most favorable atomic structure is the one with the lowest surface free energy. For example, in the case of In/GaAs, the surface energy γ can be written in the form

$$\gamma A = E_{tot} - \mu_{\mathrm{GaAs}} N_{\mathrm{As}} - (N_{\mathrm{Ga}} - N_{\mathrm{As}})\mu_{\mathrm{Ga}} - N_{\mathrm{In}}\mu_{\mathrm{In}}, \quad (1)$$

where A, E_{tot}, N_{As}, N_{Ga}, and N_{In} denote surface area, total energy, and the number of As, Ga, and In atoms, respectively, for the considered stoichiometry. Here μ_{GaAs}, μ_{Ga}, and μ_{In} are the corresponding chemical potentials for bulk GaAs, Ga, and In. The μ_{Ga} and μ_{In} act as variables in Eq. (1), and the upper limit for both chemical potentials is obtained from bulk values while the lower limit of μ_{Ga} can be deduced using the heat of formation ΔH_f of GaAs. Therefore, μ_{Ga} varies within the range,

$$\mu_{\mathrm{Ga},bulk} - \Delta H_f < \mu_{\mathrm{Ga}} < \mu_{\mathrm{Ga},bulk}. \quad (2)$$

The chemical potentials for the bulk structures were calculated by using orthorhombic[46] (Ga), tetragonal (In), and rhombohedral (As, Sb) unit cells.

III. EXPERIMENTS

The experiments were performed in an ultrahigh vacuum (UHV) system (Omicron) equipped with room-temperature (RT) STM, x-ray photoelectron spectroscopy (XPS), and low-energy electron diffraction (LEED). The samples were cut from an n-type GaAs(100) wafer and cleaned in UHV environment with cycles of argon-ion sputtering (1.5 kV and 10 mA) and subsequent indirect annealing treatment. During sputtering, the temperature of the sample was kept around 400 °C and increased to 580 °C afterward. Temperature was monitored by an infrared pyrometer. Typically, after four cycles of sputtering and annealing, LEED revealed a clear $(6\times6)+(4\times2)$ pattern for GaAs. The indium deposition was done onto this surface at RT by using Knudsen cell evaporator with quartz-crystal microbalance facilities to estimate the indium flux. After deposition of 0.5–1 ML and annealing the sample at 500 °C, LEED pattern changed to $c(8\times2)$ without any other phase. The presence of indium was confirmed by XPS measurements. The STM images were acquired in the constant-current mode. Tests showed that 1–2 ML of indium produced a similar $c(8\times2)$ LEED pattern.

IV. RESULTS AND DISCUSSION

Figure 1 shows different (4×2) atomic models considered in this work. We also calculated various In-stabilized (2×4) and clean GaAs models (not shown) to obtain a complete phase diagram for the In/GaAs(100)$c(8\times2)$ surface. The obtained diagram in Fig. 2(a) demonstrates the stability of four different ζa structures on the In/GaAs(100)$c(8\times2)$ surface: ζa1 and ζa4 [Figs. 1(d) and 1(g), respectively] and two modifications of the ζa1 with the In amounts of 1.5 and 2 ML. In these two models, the monomer rows are occupied with 100% of In together with 100% of In occupancy on atomic sites labeled 4 and 4′ in the Fig. 3(a). To present the energy differences of the models, we show in Fig. 2(b) a cross section of the phase diagram in the very In-rich limit

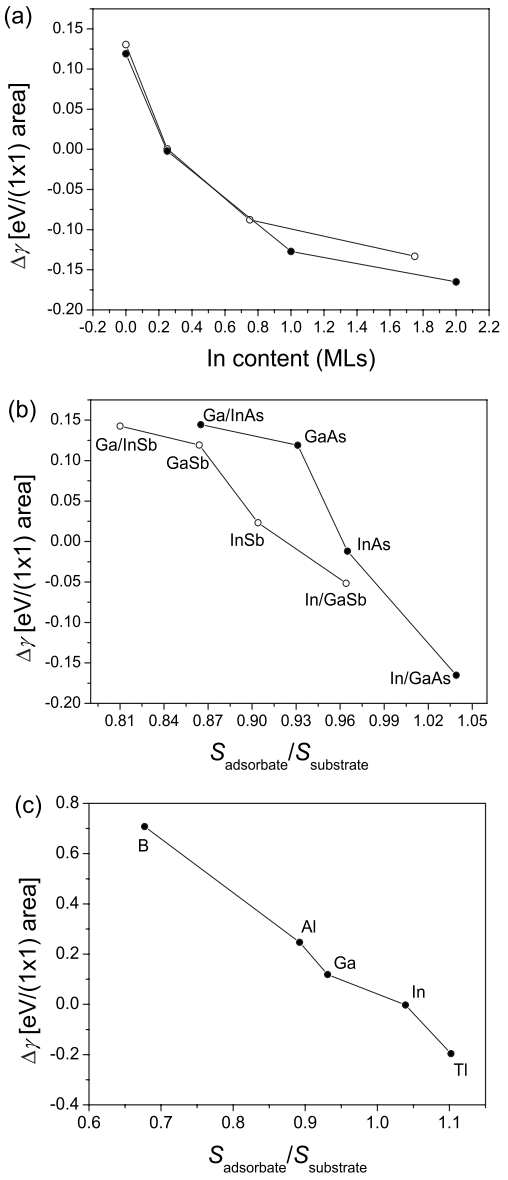

FIG. 4. (a) Surface-energy difference ($\Delta\gamma$) between ζ and ζa structures ($E_{\zeta a}-E_{\zeta}$) for In/GaAs for different In coverages (solid circles). Relative stability between the ζ structure and the ζ structure with dimer broken (atoms 4 and 4′ occupy the same positions as in the ζa structure) is also shown (open circles). The solid circles show the In content in the ζa reconstructions (ζa1 and ζa7) whereas the open circles show the In content in the ζ reconstructions (ζ and ζ2). These results correspond to the very In-rich limit ($\mu_{\mathrm{In}}-\mu_{\mathrm{In,bulk}}=0$ eV). (b) Surface-energy difference ($\Delta\gamma$) between ζ and ζa structures ($E_{\zeta a}-E_{\zeta}$) for different III/III-V surfaces as a function of the ratio of surface cation and average substrate Wigner-Seitz radii (S). Two layers of adsorbate cations are assumed in these results. Some of the points correspond to pure two-component surfaces. The results correspond to the very Ga-rich (In-rich) limit ($\mu_{\mathrm{Ga(In)}}-\mu_{\mathrm{Ga(In),bulk}}=0$ eV). (c) Surface-energy difference ($\Delta\gamma$) between ζ and ζa structures ($E_{\zeta a}-E_{\zeta}$) for III/GaAs surfaces as a function of the ratio of surface cation and average substrate Wigner-Seitz radii (S). There are adsorbate atoms only at the atom positions 4 and 4′ (0.25 ML). These results correspond to the very Ga-rich limit ($\mu_{\mathrm{Ga}}-\mu_{\mathrm{Ga,bulk}}=0$ eV).

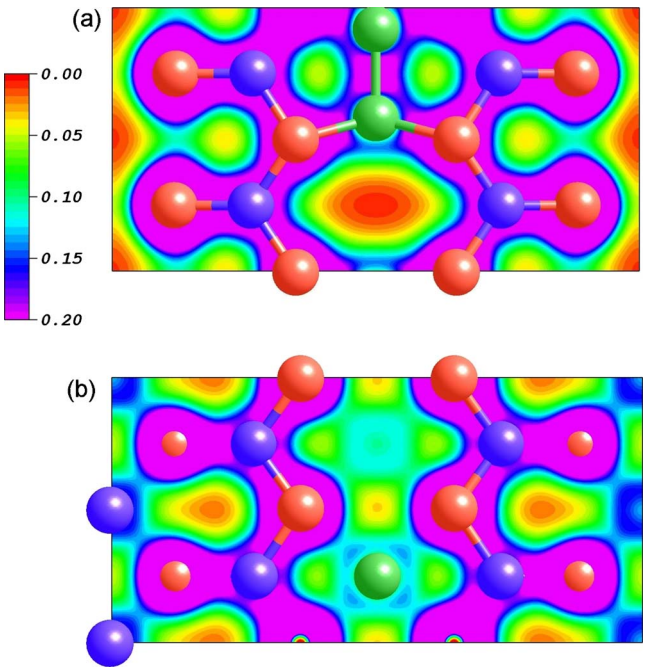

FIG. 5. (Color online) Electron density ($e/\mathrm{Å}^3$) for (a) ζ structure (plane crosses the 4 and 4′ dimer atoms) and (b) ζa structure (plane crosses the upper dimer atom 4′) of In/GaAs(100) surface (two In atoms at the atomic sites 4 and 4′).

($\mu_{\mathrm{In}}-\mu_{\mathrm{In,bulk}}=0$ eV). (The models with In concentration above 1 ML are not shown for clarity. Some especially ζ- and ζb-type models along with models including heterodimers are not included in the phase diagram and Fig. 1, either.) This energy diagram reveals a significant stability of the In/GaAs ζa structures described above. (The stability of the ζa reconstruction for any III-V semiconductor surface has not been confirmed theoretically before.) For example, the energy difference between the previously proposed ζ model [Fig. 1(a)] and the present ζa1 one is 122 meV per (1×1) surface area. The stability area of the In-induced mixed-dimer (2×4) model is clearly decreased compared to a previous theoretical study, in which the ζa structure was not considered.[47] This is consistent with experiments which show that only the $c(8\times2)$ periodicity is formed in the Ga- and/or In-rich conditions on the GaAs substrate. The above results indicate that in experiments, one should not rely only on RHEED in calibrating indium flux since the In amount between 0.5 and 2 ML leads to a similar $c(8\times2)$ RHEED pattern. Thus there is a risk that a thin InAs layer forms in the interface at higher In amounts, which is not always the goal.

Considering the ζ model, we found that it is energetically unfavorable for In atoms to dimerize along [011] direction at the atomic sites 4 and 4′ [Figs. 3(a) and 3(b)] on the In/GaAs(100) surface. It was found that by breaking this In-In bond in the ζ reconstruction and thus producing more ζa1-like structure (i.e., ζa1 excluding monomer rows), the surface-energy reduction was 0.07 eV per (1×1) surface area (this energy change was obtained by comparing the total energies of the ζ structure and the "nondimerized ζ structure" calculated self-consistently) in spite of the fact, that this

TABLE I. Formal ionic charges for the atoms shown in Fig. 3. Charges in the sets ζ^* and ζa^* were obtained by omitting the bond between atoms 3 and 5 (and 3′ and 5′).

	2,2′	4,4′	9,9′	5,5′	7,7′	1,1′	3,3′	6,6′	8,8′
ζ	0.75	0.50		−0.25	0.00	−0.75	0.00	0.00	0.00
ζ^*	0.75	0.50		0.50	0.00	−0.75	−0.75	0.00	0.00
ζa	0.75	0.50	0.50	−0.25	0.00	−0.75	−0.25	0.00	0.00
ζa^*	0.75	0.50	0.50	0.50	0.00	−0.75	−1.00	0.00	0.00

modified structure does not obey the electron counting model (ECM).[48] Furthermore, this surface-energy reduction increases as the In content is increased, which is shown in Fig. 4(a) together with the corresponding energy difference between the ζ and ζa structures. One can note that the curves are quite similar.

Next, we consider the energy difference between the ζ and ζa structures by changing the group III adsorbate (Ga and In) and the substrate (GaAs, InAs, GaSb, and InSb). The Wigner-Seitz (W-S) radii for ground-state bulk Ga and In are 1.625 Å and 1.814 Å, respectively. The average W-S radii for ground-state bulk GaAs, InAs, GaSb, and InSb are 1.746 Å, 1.879 Å, 1.881 Å, and 2.007 Å, respectively. Figure 4(b) shows the energy difference as a function of the ratio of the adsorbate and average substrate W-S radii for two different substrate anion atoms (As and Sb) in the group III atom-rich conditions. In these calculations, two uppermost surface layers were filled up by the adsorbate atoms (corresponding to 1.75 or 2 ML of adsorbate). These results show a clear trend. The larger is the considered ratio, the larger is the energy difference in favor of the ζa reconstruction. It is also noted that the energy difference between the ζ and ζa reconstructions is quite small for InAs and InSb while the ζ reconstruction is clearly the more stable phase for GaAs. These results agree with the experimental results of Kumpf *et al.*[27] (Table II in Ref. 27) according to which GaAs shows more ζ-type local configurations whereas InAs shows more ζa-type local configurations (InSb shows significantly both types of local configurations). We note that Miwa *et al.* obtained that the ζ reconstruction is stable for the InAs using pseudopotentials.[28] To get a wider view of the considered phenomena, Fig. 4(c) shows the surface-energy difference between the ζ and ζa for cases in which only two adsorbate cation atoms occupy the atomic sites 4 and 4′ on GaAs. However, now also small B and Al atoms and the large Tl atom are included. These results show the same tendency as the previous results. In conclusion, as the adsorbate atom size is increased, the ζa reconstruction is stabilized. This effect gets stronger as the amount of the adsorbate atoms is increased. Thus we propose that in future experiments, the B-, Al-, and Tl-induced reconstructions are studied in order to confirm the above results.

The ζa structure is peculiar because some of the group III atoms do not have any close neighbors, and they do not form strong covalent bonds, which are characteristic for the bulk semiconductors and semiconductor surfaces. Figure 5 shows electron densities for a plane parallel to surface for ζ and ζa reconstructions of In/GaAs(100) with two In atoms at atom sites 4 and 4′. It is easy to see that in the ζa structure, there is no significant electron density between the In atoms and the neighboring As atoms, and therefore no covalent bonds. On the other hand, the In atoms in the ζ structure clearly form covalent bonds with the neighboring As atoms. The ζa phase is stabilized significantly relative to the ζ phase upon In adsorption (two In atoms) [about 0.12 eV per (1×1) area]. The density of states curves do not reveal any significant changes upon adsorption. Therefore, we assume that the ζa stabilization has an electrostatic origin. We calculated Madelung energies for these surfaces,

$$E = -\frac{1}{2}\sum_{i,j,i\neq j}\frac{q_i \cdot q_j}{|\bar{r}_i - \bar{r}_j|}, \tag{3}$$

where we used different formal ionic charges[49,50] (q_i) for the ions (keeping the overall charge neutrality). The vectors r_i denote the positions of the atoms. The Madelung energy was calculated using Ewald's technique. It is important to remember that the charges in the Eq. (3) are ionic charges (i.e., sums of the negative electronic charges and positive nucleus charges) not electronic charges. These formal charges are determined on the basis of the octet rule and ECM (Ref. 48) (or electron counting rule). In bulk, the octet rule is satisfied, when all group III atoms donate 3/4 electrons for every bond and all group V atoms donate 5/4 electrons for every bond. There are four bonds per atom. On the surface, one has to take into account also dimer bonds and dangling bonds. If the number of bonds is less than four for some atom, then that atom has a dangling bond. According to the electron counting model, this bond is occupied for group V atoms giving two electrons to them whereas the dangling bond of a group III atom is empty. In the considered case, there are only homodimer bonds, which imply one electron per dimer atom. Using these rules, one can count electronic charge (which has a minus sign) for a surface atom, from which the electronic charge of neutral atom is substracted. This result is the formal ionic charge for an atom. Screening is taking into account by diving the energy from the Eq. (3) by the static dielectric constant (which is ~13 for GaAs).[49,50]

The surface structure in the first layer of the ζ and ζa reconstructions is quite peculiar because the first Ga (group III) and As (group V) atomic layers are intermixed. Therefore, it is not so straightforward to determine which atomic pairs show bonds. However, the electron charge densities between different atoms on the surface were calculated, and from these results the bonds could be determined. The found bonds are shown in Fig. 3. Using this characterization, we determined the formal ionic charges, which are shown in Table I. We also used another set of formal ionic charges to

TABLE II. Madelung energy changes [electron volt per (1×1) area] for different III/GaAs surfaces. First rows show results for the surfaces with 0.25–2.00 ML of In and 0.25 ML of B, Al, and Tl. Last rows show results for In/GaAs surfaces with 0.25 and 2.00 ML of In. In these calculations, the ionic formal charges are modified compared to those in Table I. The anion ionic formal charges q_3 are decreased by $0.25e-1.00e$. This increased negative charge is compensated by increasing the positive formal charges of atoms 4 and 9 (and 4′ and 9′).

	ζ	ζa	ζ^*	ζa*
0.25 ML In	0.000	0.004	0.000	−0.003
0.75 ML In	0.018		0.020	
1.00 ML In		0.023		0.019
1.75 ML In	0.020		0.030	
2.00 ML In		0.023		0.029
0.25 ML B	0.013	−0.005	−0.029	0.011
0.25 ML Al	−0.001	−0.002	−0.002	−0.002
0.25 ML Ga	0.0	0.0	0.0	0.0
0.25 ML In	0.000	0.004	0.000	−0.003
0.25 ML Tl	0.004	0.006	−0.004	−0.005
0.25 ML In				
$\Delta q_3=-0.25e$	−0.050	−0.091	−0.090	−0.139
$\Delta q_3=-0.50e$	−0.138	−0.208	−0.217	−0.298
$\Delta q_3=-1.00e$	−0.425	−0.507	−0.583	−0.679
1.75 or 2.00 ML In				
$\Delta q_3=-0.25e$	−0.032	−0.072	−0.053	−0.101
$\Delta q_3=-0.50e$	−0.120	−0.187	−0.172	−0.252
$\Delta q_3=-1.00e$	−0.403	−0.482	−0.518	−0.618

be assured that the results are not sensitive to the specific choice of the formal charges. This set was obtained by assuming that there is no bond between the atoms 3 and 5 (and 3′ and 5′) in Fig. 3. The formal ionic charges for the ζa reconstruction can be obtained as for the ζ reconstruction except for the atoms 4 and 9 because they do not show covalent bonds. For the atoms 4, the same ionic formal charge is chosen as in the ζ structure, which is also used for the atoms 9. Then the formal charge of the atoms 3 in the ζa structure is obtained by using the charge neutrality. The resulting formal charges for the atoms 3, 4, and 9 (or atoms in the first layer) in the ζa reconstruction are to a some extent arbitrary (but similar to those in the ζ reconstruction) but it turns out that the effects found below depend only slightly on the initial choices of the formal ionic charges.

Madelung energy calculations show that it is not possible to explain found large total-energy changes, induced, e.g., by In adsorption, assuming constant ionic charges for the group III atoms (e.g., Ga and In), by changes in Madelung energy. Table II shows Madelung energy differences between the pure GaAs surface and different adsorbate systems (0.25–2.00 ML In on the GaAs surface and 0.25 ML different group III atoms on the GaAs surface). The Madelung energy differences are very small compared to the found total-energy differences upon adsorption. This means that significant energy changes upon adsorption cannot be explained by a Madelung energy change due to a structural change. Because the atoms 4 and 9 (and 4′ and 9′) do not show strong covalent bonds, instead they seem to indicate more metallic bonds with spherical electron densities (these atoms show much smaller electronic charges than all the other atoms in both structures within equal-sized spheres due to the missing covalent bonds), we expect that the stabilization of the ζa upon In adsorption (In atoms at the "metallic" sites 4 and 4′) is partly due to a changed Madelung energy caused by increased ionicity. Using Eq. (3), we find that the Madelung energy is lowered significantly, if, e.g., the ionicity of the atoms 3 and 4 is increased (the group III atoms 4 and 4′ and the neighboring group V atoms). Table II shows Madelung energy changes for cases, in which the anion formal charges for atoms 3 are $0.25e-1.00e$ more negative. (Results are changed only a little, if the increased negative ionicity is distributed between the atoms 1 and 3.) This increased negative charge is compensated by increasing the positive charge of the cations 4 and 4′ (and 9 for ζa). It is expected that the peculiar metallic nature of the bonds for atoms 4 and 4′ in the ζa reconstruction increases ionicity, especially for larger group III atoms (In and Tl), which distribute electronic charge in larger volumes. Furthermore, the electronegativity decreases in group III as the volume of the group III atom increases Al being an exception in this trend with an exceptionally low electronegativity value [electronegativities: 2.04 (B), 1.61 (Al), 1.81 (Ga), In (1.78), and 1.62 (Tl)]. While the electronic charges in atomic spheres cannot straightforwardly linked to ionic charges, the electronic charges in the As atoms 3 for surfaces with 0.25 ML of different group III adsorbate atoms are shown in Table III. The amount of the electronic charge is increased (decreased) in equal-sized spheres around As atoms 3 for the ζa (ζ) reconstruction Al being an exception. For larger adsorbate coverages, it is even more difficult to estimate ionicities from electronic charges because the volume in the surface layer is changed. One cannot compare the electronic charges of nonequivalent atom types due to their different volumes. Our results show that, e.g., the stabilization of the ζa reconstruction upon In adsorption is in comparable magnitudes due to both the increase in the surface energy of ζ and decrease in the surface energy of ζa. The $\Delta\gamma$ between B/GaAs and GaAs from Fig. 4(c) is about 0.6 eV/(1×1) area. If, e.g., half of this surface-energy change would be due to the Madelung energy change in the ζa surface due to the larger ionicity of B compared to that of Ga, one can estimate from Table II that the Δq_3 should be larger than $-0.5e$. This would correspond to a real

TABLE III. Electronic charges (e) in As atomic spheres 3 (Fig. 3) for III/GaAs surface with 0.25 ML of adsorbate (B, Al, Ga, In, and Tl). The radii of the As spheres are 1.217 and 1.400 Å.

	ζ	ζa	ζ	ζa
B/GaAs	2.864	2.766	3.862	3.693
Al/GaAs	2.837	2.798	3.793	3.732
GaAs	2.820	2.794	3.763	3.719
In/GaAs	2.800	2.804	3.756	3.734
Tl/GaAs	2.809	2.809	3.738	3.740

TABLE IV. Selected interatomic distances (Å) in ζ and ζa structures of the In/GaAs(100) surface for different In coverages (0.25–2.00 ML). Atom positions are the same as in Fig. 3.

	ζ				ζa			
	0 ML	0.25 ML	0.75 ML	1.75 ML	0 ML	0.25 ML	1 ML	2 ML
2-3	2.44	2.43	2.59	2.59	2.44	2.43	2.58	2.58
1-2	2.35	2.34	2.53	2.54	2.41	2.40	2.56	2.56
1′-2′	2.37	2.35	2.51	2.53	2.44	2.42	2.59	2.59
2′-3	2.46	2.43	2.59	2.61	2.48	2.47	2.62	2.63
4-4′	2.43	2.68	2.65	2.65	3.99	4.02	3.92	4.03
4-3′	2.46	2.61	2.59	2.61	3.04	3.14	3.02	3.03
1-7′	2.45	2.45	2.45	2.60	2.49	2.49	2.49	2.65
1′-7	2.46	2.46	2.48	2.62	2.49	2.49	2.49	2.64
7-8	2.47	2.45	2.43	2.58	2.45	2.44	2.42	2.57
5-6	2.41	2.41	2.43	2.55	2.44	2.44	2.46	2.59
5-5′	2.53	2.50	2.48	2.73	2.57	2.55	2.55	2.82

electronic charge change larger than $-0.038e$. One can see from Table III that this electronic charge change in spheres around atoms 3 having radius of 1.217 Å is $-0.028e$. It is concluded that the Madelung energy change explains a significant portion of the total-energy change upon adsorption.

On the other hand, larger group III atoms cause structural strain. It is supposed that this is true especially in the ζ structure, which destabilizes this reconstruction. This is also an electrostatic effect but not necessarily fully taken into account by the Madelung energy. This phenomenon is supposed to be strengthened as the adsorbate coverage is increased. Table IV shows some interatomic distances for the surface atoms in the ζ and ζa structures for different In coverages (from 0 to 2 ML). One can note, e.g., changes in the 2′-3 and 5-5′ bond lengths with 0.25 ML In coverage, which are larger for the ζ reconstruction than for the ζa reconstruction (2′-3 being a Ga-As bond and 5-5′ being a Ga-Ga bond in both cases for this coverage).

The STM images are representations of the charge-density distribution, and therefore, they should be considered with care, when it is tried to identify the atomic positions. Some progress can be achieved by comparing the experimental STM images with the theoretical STM images calculated for selected surface structures. Theoretically obtained filled-state STM images of the ζ1, ζa1, ζb2, α2, β2-2, β2-3, and β3′-2 models are shown in Fig. 6. It is worth noting that similar images were found for any of the other possible atomic configurations constructed on the basis of the basic ζ1, ζa1, ζb2, α2, β2-2, β2-3, and β3′-2 geometries. The latter four models can be readily ruled out by comparing with the previously measured filled-state STM image in Ref. 35. The ζ1 model can be also excluded since its image does not include any dark rows between the white and nearest gray ones, which are clearly seen in experiment.[35] In contrast, the calculated filled-state images for the ζa and ζb models agree well with our measured image in Fig. 7(a) together with previous STM studies[35] showing faint gray protrusions between bright rows along [011] direction. According to our results, these faint features originate from threefold-coordinated As atoms at sites 3 and 3′ when bright [011] directed rows stem from In monomer rows. It can be, however, seen that the ζa and ζb structures cannot be well distinguished on the basis of the filled-state STM images.

In Fig. 7(b), we present the measured empty-state image which allows making separation between the ζa and ζb models. It clearly shows gray protrusions with a double periodicity along the [011] direction, which are located between the bright white rows. Obviously, such corrugation is well consistent with the ζa model of which empty-state image is shown in Fig. 7(h). In contrast, the images in Figs. 7(f) and 7(g) are inconsistent with that of Fig. 7(b). Previous experimental study of Xue *et al.* also reported hump-plus-line features in empty-state STM images, however, no theoretical support has been reported.[23,51] This 2× feature in calculated ζa STM images originate from In atom on top of the subsurface dimer at atomic site 4′ in Fig. 3(a). The In atom protrudes strongly outward holding almost the same z coordinate as surrounding As atoms while In atom at site 4 holds much lower position. This is consistent with experiments which show small buckling between the atomic sites in question on In/GaAs(100) surface.[32] The simulated empty-state

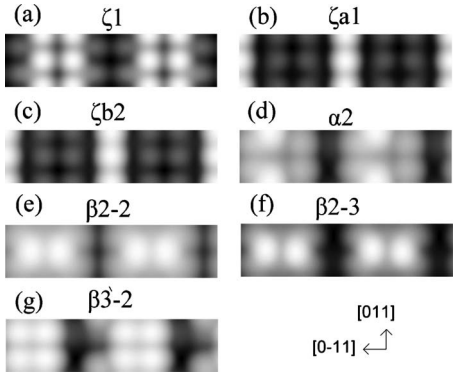

FIG. 6. Calculated STM images of the (a) ζ1, (b) ζa1, (c) ζb2, (d) α2, (e) β2-2, (f) β2-3, and (g) β3′-2 models at the filled-state voltage of 2.20 V.

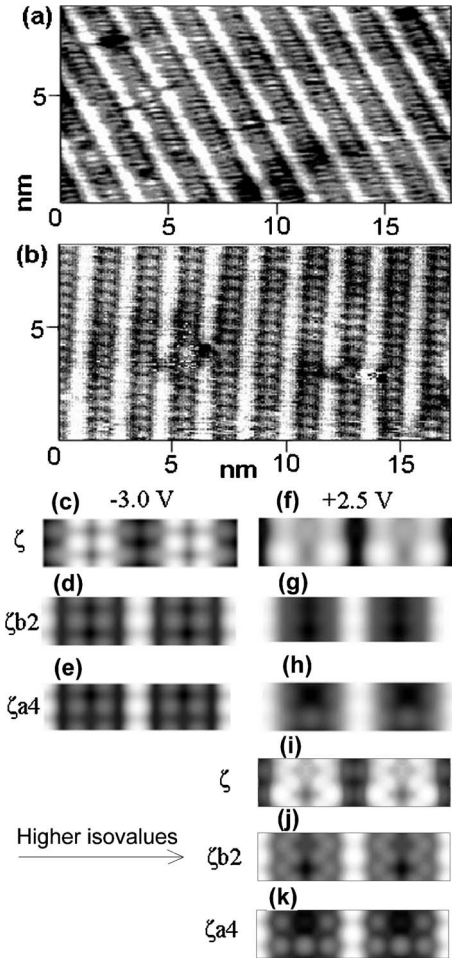

FIG. 7. (a) Measured filled-state STM image of the In/GaAs(100)$c(8\times2)$ surface; tunneling current $I=0.16$ nA, and voltage $V=3.05$ V. (b) Measured empty-state image of the In/GaAs(100)$c(8\times2)$ surface, $I=0.02$ nA, and $V=2.54$ V. (c)–(e) Calculated filled-state STM images (3.00 V) for the ζ, ζb2, and ζa4 models. Charge-density isovalue is 4.5×10^{-5} $e/\text{Å}^3$. (f)–(h) Calculated empty-state STM images (2.50 V) for the ζ, ζb2, and ζa4 models. Charge-density isovalue is 4.5×10^{-5} $e/\text{Å}^3$. (i)–(k) Calculated empty-state STM images (2.50 V) for the ζ, ζb2, and ζa4 models. Charge-density isovalue is 2.5×10^{-3} $e/\text{Å}^3$.

images for considered models in Fig. 7 are calculated using two different isovalues for the constant charge density in the STM (constant-current mode) because the empty-state images are more sensitive to the choice of the isovalue than the filled-state images, which may be due to smaller height differences in the empty-state images.

V. CONCLUSIONS

The present first-principles results reveal an interesting trend. The relative stability of the peculiar ζ and ζa structures of the III-V(100)$c(8\times2)$ surface depends strongly on the surface-layer cation size and the substrate volume. The stability of the ζa reconstruction is increased as the surface-layer cation size is increased and/or the substrate volume is decreased. This phenomenon is related to the peculiar metallic-type group III atoms in the ζa structure, and the strain induced especially in the ζ structure, when large cations are adsorbed. Our theoretical results predict a phase transition at 0 K upon adsorption for many systems, e.g., for GaAs upon In adsorption. It is probable that the small surface-energy difference between the ζ and ζa reconstructions for InAs and InSb [Fig. 4(b)] explains the experimentally found disorder at room temperature for these phases.[26,27] (Our previous studies show that energy differences of this magnitude can be compensated by configurational entropy at room temperature.[52,53]) We propose that the ionicity is increased and the Madelung energy of the surface is decreased, as the size of these metallic-type cations is increased. On the other hand, the larger cations increase the strain especially in the ζ structure, which includes an additional dimer in the surface layer, which destabilizes the ζ structure as the cation size is increased. As a detailed example, our first-principles phase diagrams demonstrate the significant stability of the $c(8\times2)$-ζa structures with the 0.5, 1, 1.5, and 2 ML In coverages on the GaAs(100) substrate. This finding is supported by the comparison of the calculated STM images with the former and present STM measurements.

ACKNOWLEDGMENTS

We are grateful to H. Ollila for his technical assistance. The calculations were performed using the facilities of the Finnish Centre for Scientific Computing (CSC) and the Mgrid project (Turku, Finland). The Swedish Research Council (L.V and B.J.), the Swedish Foundation for Strategic Research (L.V. and B.J.), the National Graduate School in Materials Physics (J.L.), Solar III-V project (Dnro: 3120/31/08), the Carl Tryggers Foundation (M.P.J.P.), the Turku University Foundation (M.P.J.P.), and the Emil Aaltonen Foundation (M.P.J.P.) are also acknowledged for financial support. This work has been supported by the Academy of Finland under Grants No. 122743 (P.L.) and No. 122355 (I.J.V.) as well as Finnish Academy of Sciences and Letters (P.L.).

*Corresponding author; jjklan@utu.fi

[1] T. Anan, S. Sugou, and K. Nishi, Appl. Phys. Lett. **63**, 1047 (1993).
[2] Q. Xue, T. Hashizume, and T. Sakurai, Prog. Surf. Sci. **56**, 1 (1997).
[3] W. G. Schmidt, Appl. Phys. A **75**, 89 (2002).
[4] P. Kratzer, E. Penev, and M. Scheffler, Appl. Surf. Sci. **216**, 436 (2003).
[5] S. Froyen and A. Zunger, Phys. Rev. B **53**, 4570 (1996).
[6] B. Z. Nosho, W. H. Weinberg, W. Barvosa-Carter, B. R. Bennet,

B. V. Shanabrook, and L. J. Whitman, Appl. Phys. Lett. **74**, 1704 (1999).
[7] C. L. Hinkle, A. M. Sonnet, E. M. Vogel, S. McDonnel, G. J. Hughes, M. Milojevic, B. Lee, F. S. Aguirre-Tostado, K. J. Choi, H. C. Kim, J. Kim, and R. M. Wallace, Appl. Phys. Lett. **92**, 071901 (2008).
[8] N. Goel, P. Majhi, C. O. Chui, W. Tsai, D. Choi, and J. S. Harris, Appl. Phys. Lett. **89**, 163517 (2006).
[9] P. T. Chen, Y. Sun, E. Kim, P. C. McIntyre, W. Tsai, M. Garner, P. Pianetta, Y. Nishi, and C. O. Chui, J. Appl. Phys. **103**, 034106 (2008).
[10] H. L. Lu, L. Sun, S. J. Ding, M. Xu, D. W. Zhang, and L. K. Wang, Appl. Phys. Lett. **89**, 152910 (2006).
[11] S. Oktyabrsky, V. Tokranov, M. Yakimov, R. Moore, S. Koveshnikov, W. Tsai, F. Zhu, and J. C. Lee, Mater. Sci. Eng., B **135**, 272 (2006).
[12] B. J. Skromme, C. J. Sandroff, E. Yablonovitch, and T. Gmitter, Appl. Phys. Lett. **51**, 2022 (1987).
[13] H. Hasegawa, H. Ishii, T. Sawada, T. Saitoh, S. Konishi, Y. Liu, and H. Ohno, J. Vac. Sci. Technol. B **6**, 1184 (1988).
[14] H. Hasegawa, M. Akazawa, H. Ishii, and K. Matsuzaki, J. Vac. Sci. Technol. B **7**, 870 (1989).
[15] M. J. Hale, J. Z. Sexton, D. L. Winn, A. C. Kummel, M. Erbudak, and M. Passlack, J. Chem. Phys. **120**, 5745 (2004).
[16] H.-S. Kim, I. Ok, M. Zhang, F. Zhu, S. Park, J. Yum, H. Zhao, J. C. Lee, P. Majhi, N. Goel, W. Tsai, C. K. Gaspe, and M. B. Santos, Appl. Phys. Lett. **93**, 062111 (2008).
[17] B. Shin, D. Choi, J. S. Harris, and P. C. McIntyre, Appl. Phys. Lett. **93**, 052911 (2008).
[18] J. Schmitz, J. Wagner, F. Fuchs, N. Herres, P. Koidl, and J. D. Ralston, J. Cryst. Growth **150**, 858 (1995).
[19] Q. Xue, T. Ogino, H. Kiyama, Y. Hasegawa, and T. Sakurai, J. Cryst. Growth **175-176**, 174 (1997).
[20] F. Maeda, M. Sugiyama, and Y. Watanabe, Phys. Rev. B **62**, 1615 (2000).
[21] P. B. Joyce, T. J. Krzyzewski, G. R. Bell, B. A. Joyce, and T. S. Jones, Phys. Rev. B **58**, R15981 (1998).
[22] P. B. Joyce, T. J. Krzyzewski, G. R. Bell, T. S. Jones, S. Malik, D. Childs, and R. Murray, Phys. Rev. B **62**, 10891 (2000).
[23] Q. K. Xue, Y. Hasegawa, T. Ogino, H. Kiyma, and T. Sakurai, J. Vac. Sci. Technol. B **15**, 1270 (1997).
[24] P. C. McIntyre, Y. Oshima, E. Kim, and K. C. Saraswat, Microelectron. Eng. **86**, 1536 (2009).
[25] S.-H. Lee, W. Moritz, and M. Scheffler, Phys. Rev. Lett. **85**, 3890 (2000).
[26] C. Kumpf, L. D. Marks, D. Ellis, D. Smilgies, E. Landemark, M. Nielsen, R. Feidenhans'l, J. Zegenhagen, O. Bunk, J. H. Zeysing, Y. Su, and R. L. Johnson, Phys. Rev. Lett. **86**, 3586 (2001).
[27] C. Kumpf, D. Smilgies, E. Landemark, M. Nielsen, R. Feidenhans'l, O. Bunk, J. H. Zeysing, Y. Su, R. L. Johnson, L. Cao, J. Zegenhagen, B. O. Fimland, L. D. Marks, and D. Ellis, Phys. Rev. B **64**, 075307 (2001).
[28] R. H. Miwa, R. Miotto, and A. C. Ferraz, Surf. Sci. **542**, 101 (2003).
[29] D. Paget, Y. Garreau, M. Sauvage, P. Chiaradia, R. Pinchaux, and W. G. Schmidt, Phys. Rev. B **64**, 161305 (2001).
[30] P. De Padova, C. Quaresima, P. Perfetti, R. Larciprete, R. Brochier, C. Richter, V. Ilakovac, P. Bencok, C. Teodorescu, V. Y. Aristov, R. L. Johnson, and K. Hricovini, Surf. Sci. **482-485**, 587 (2001).
[31] A. Ohtake, S. Tsukamoto, M. Pristovsek, N. Koguchi, and M. Ozeki, Phys. Rev. B **65**, 233311 (2002).
[32] T.-L. Lee, C. Kumpf, A. Kazimirov, P. F. Lyman, G. Scherb, M. J. Bedzyk, M. Nielsen, R. Feidenhans'l, R. L. Johnson, B. O. Fimland, and J. Zegenhagen, Phys. Rev. B **66**, 235301 (2002).
[33] J. J. Kolodziej, B. Such, M. Szymonski, and F. Krok, Phys. Rev. Lett. **90**, 226101 (2003).
[34] H. Xu, Y. Y. Sun, Y. G. Li, Y. P. Feng, A. T. S. Wee, and A. C. H. Huan, Phys. Rev. B **70**, 081313 (2004).
[35] U. Resch-Esser, N. Esser, C. Springer, J. Zagenhagen, W. Richter, M. Cardona and B. O. Fimland, J. Vac. Sci. Technol. B **13**, 1672 (1995).
[36] D. M. Ceperley and B. J. Alder, Phys. Rev. Lett. **45**, 566 (1980).
[37] J. P. Perdew and A. Zunger, Phys. Rev. B **23**, 5048 (1981).
[38] P. E. Blöchl, Phys. Rev. B **50**, 17953 (1994).
[39] G. Kresse and D. Joubert, Phys. Rev. B **59**, 1758 (1999).
[40] G. Kresse and J. Hafner, Phys. Rev. B **47**, 558 (1993).
[41] G. Kresse and J. Hafner, Phys. Rev. B **49**, 14251 (1994).
[42] G. Kresse and J. Furthmüller, Comput. Mater. Sci. **6**, 15 (1996).
[43] G. Kresse and J. Furthmüller, Phys. Rev. B **54**, 11169 (1996).
[44] H. J. Monkhorst and J. D. Pack, Phys. Rev. B **13**, 5188 (1976).
[45] J. Tersoff and D. R. Hamann, Phys. Rev. Lett. **50**, 1998 (1983); Phys. Rev. B **31**, 805 (1985).
[46] M. Bernasconi, G. L. Chiarotti, and E. Tosatti, Phys. Rev. B **52**, 9988 (1995).
[47] A. Jenichen and C. Engler, Surf. Sci. **601**, 900 (2007).
[48] M. D. Pashley, Phys. Rev. B **40**, 10481 (1989).
[49] W. G. Schmidt, S. Mirbt, and F. Bechstedt, Phys. Rev. B **62**, 8087 (2000).
[50] J. E. Northrup and S. Froyen, Phys. Rev. B **50**, 2015 (1994).
[51] R. H. Miwa, R. Miotto, A. C. Ferraz, and G. P. Srivastava, Phys. Rev. B **67**, 045325 (2003).
[52] P. Laukkanen, M. P. J. Punkkinen, N. Räsänen, M. Ahola-Tuomi, M. Kuzmin, J. Lång, J. Sadowski, J. Adell, R. E. Perälä, M. Ropo, K. Kokko, L. Vitos, B. Johansson, M. Pessa, and I. J. Väyrynen, Phys. Rev. B **81**, 035310 (2010).
[53] M. P. J. Punkkinen, M. Kuzmin, P. Laukkanen, R. E. Perälä, M. Ahola-Tuomi, J. Lång, M. Ropo, M. Pessa, I. J. Väyrynen, K. Kokko, B. Johansson, and L. Vitos, Phys. Rev. B **80**, 235307 (2009).